Published in final edited form as:
Invest Ophthalmol Vis Sci. 2008 October ; 49(10): 4631–4640. doi:10.1167/iovs.07-1224.

Age-Related Cone Abnormalities in Zebrafish with Genetic Lesions in Sonic Hedgehog

Deborah L. Stenkamp[1], **Rosanna Satterfield**[1], **Kalyani Muhunthan**[1], **Tshering Sherpa**[1], **Thomas S. Vihtelic**[2], and **David A. Cameron**[3]

1*Department of Biological Sciences, University of Idaho, Moscow, Idaho*

2*Department of Biological Sciences, and Center for Zebrafish Research, University of Notre Dame, Notre Dame, Indiana*

3*Department of Neuroscience and Physiology, State University of New York Upstate Medical University, Syracuse, New York*

Abstract

Purpose—Sonic hedgehog (Shh) signaling is essential for photoreceptor differentiation and retinal cell survival in embryonic zebrafish. The study was conducted to determine whether adult heterozygous carriers of mutant alleles for the *shh* gene display retinal abnormalities.

Methods—Retinal cryosections from young, middle-aged, and senescent wild-type and sonic-you$^{+/-}$ (*syu*$^{+/-}$) zebrafish were probed with retinal cell type–specific markers. Contralateral retinal flatmounts from these fish, and from adult albino zebrafish subjected to light-induced photoreceptor damage followed by regeneration, were hybridized with blue cone opsin cRNA for quantitative analysis of the blue cone pattern. Retinal expression of *shh* mRNA was measured by quantitative RT-PCR.

Results—Regions of cone loss and abnormal cone morphology were observed in the oldest *syu*$^{+/-}$ zebrafish, although no other retinal cell type was affected. This phenotype was age-related and genotype-specific. Cone distribution in the oldest *syu*$^{+/-}$ zebrafish was predominantly random, as assessed by measuring the short-range pattern, whereas that of wild-type fish and the younger *syu*$^{+/-}$ zebrafish was statistically regular. A measure of long-range pattern revealed atypical cone aggregation in the oldest *syu*$^{+/-}$ zebrafish. The light-treated albino zebrafish displayed random cone patterns immediately after light toxicity, but showed cone aggregation on regeneration. Retinas from the *syu*$^{+/-}$ fish showed reduced expression of *shh* mRNA compared with those of wild-type siblings.

Conclusions—The *syu*$^{+/-}$ zebrafish presents a model for the study of hereditary age-related cone abnormalities. The *syu*$^{+/-}$ retinas most likely experience progressive cone photoreceptor loss, accompanied by cone regeneration. Shh signaling may be required to maintain cone viability throughout life.

The extracellular signaling molecule, Sonic hedgehog (Shh),plays multiple roles in the morphogenesis of the vertebrate eye, and regulates proliferation, differentiation, and survival of retinal cells.[1,2] During retinal development, Shh is synthesized by retinal ganglion cells[3-5] and amacrine cells.[6] The retinal pigmented epithelium (RPE) is also a source of Hedgehog signals: *shh* and tiggy-winkle hedgehog (*twhh*) in the zebrafish[7]; banded hedgehog

Corresponding author: Deborah L. Stenkamp, Department of Biological Sciences, University of Idaho, Moscow, ID 83844-3051; dstenkam@uidaho.edu.

Disclosure: D.L. Stenkamp, None; R. Satterfield, None; K. Muhunthan, None; T. Sherpa, None; T.S. Vihtelic, None; D.A. Cameron, None

(*bhh*) and cephalic hedgehog (*chh*) in *Xenopus*[8]; and Indian hedgehog (*Ihh*) in the rat.[9] Hedgehog proteins emanating from these sources influence the development of rod photoreceptors. For example, treatment of cultured rat embryonic retinal cells with recombinant Shh promotes the expression of rod photoreceptor–specific genes.[9] In addition, Shh stimulates proliferation of rat Müller glia and the generation of rhodopsin-expressing cells in vitro, and in vivo subsequent to retinal damage.[10] However, experiments using mouse retinal explants demonstrated that Shh inhibits rhodopsin synthesis,[11] suggesting the role of Shh in rod differentiation is complex and may be species-specific.

The use of anamniote vertebrate models has uncovered important roles for Hedgehog signaling in the development of rod and cone photoreceptors and the RPE. In zebrafish embryos, reduction in Shh signaling through molecular, pharmacologic, or genetic techniques results in multiple retinal abnormalities including reduced rod and cone photoreceptor differentiation.[6,7,12,13] Homozygous sonic-you ($syu^{-/-}$) mutant zebrafish,[14] display extensive retinal cell death before embryonic mortality.[13] In *Xenopus* embryos, Hedgehog signaling is necessary for RPE differentiation and maintenance.[8] Thus, in addition to regulating progenitor cell proliferation and photoreceptor differentiation, Hedgehog signaling may function in the survival and maintenance of retinal and RPE cells.

Many inherited retinal degenerative diseases, including those related to age, are characterized by rod and/or cone photoreceptor death.[15] The underlying genetic causes of many of these disorders are known and mostly involve photoreceptor-specific genes.[16,17] Murine models of inherited retinal degenerations have been valuable both in uncovering mechanisms driving photoreceptor loss and in searching for therapeutic interventions.[18] As a complement to the mouse models, zebrafish offer several advantages for studying retinal disorders. For example, zebrafish have a duplex retina with a substantial number of cone photoreceptors arranged in a precise mosaic that can be quantitatively assessed.[19,20] In addition, zebrafish are amenable to large-scale genetic manipulation.[21,22] As an example of their experimental power, the recent characterization of a zebrafish model for choroideremia, an X-linked retinal degeneration, revealed that the loss of photoreceptors in larval fish is a secondary consequence of defects in the RPE.[23]

Zebrafish are also a model for aging and age-related disease.[24,25] Their lifespan and generation time are relatively short, and potential disease treatments can be administered systemically through the water, which allows for convenient pharmacologic screening. In addition, zebrafish exhibit extraordinary neuronal regeneration, including the retinal photoreceptors, making them an excellent adult model for the study of regenerative therapies for acute disease or genetic conditions.[22,26,27] In addition, new zebrafish models of adult-onset retinal degenerations recently have been identified and characterized.[28,29] Zebrafish, however, have not yet been used to study retinal disorders associated with senescence, defined herein as the postreproductive portion of the lifespan.

In the present study, we tested the hypothesis that Hedgehog signaling is important for the maintenance and survival of photoreceptor cells throughout life. We report a novel zebrafish cone photoreceptor phenotype related to organismal senescence in heterozygous animals carrying a single mutant allele of the *shh* gene ($syu^{+/-}$), and with correspondingly lower levels of *shh* expression in the retina. The retinas of the aging $syu^{+/-}$ zebrafish display cone loss, abnormalities of cone morphology, and significant disruptions in cone organization. These disruptions in the cone mosaic are quantitatively similar to those of the light-treated and regenerated zebrafish retina, suggesting that $syu^{+/-}$ retinas exhibit a compensatory cone replacement along with cone loss.

Methods

Animals, BrdU Cell Labeling, and Light Treatments

All experiments involving animals conformed to the ARVO Statement for the Use of Animals in Ophthalmic and Visual Research. Heterozygous carriers of two different sonic you (*syu*) alleles were obtained from Anand Chandrasekhar (University of Missouri, Columbia, MO), the Zebrafish International Resource Center (*syu*^{t4}; Eugene, OR), or Rolf Karlstrom (*syu*^{tbx}; University of Massachusetts, Amherst, MA). The *syu*^{t4} allele is a deletion spanning the entire *shh* coding region as well as 4 and 2.2 kb of 5′ and 3′ flanking sequence, respectively.[14] The *syu*^{tbx} allele is null and is caused by a point mutation in the *shh* gene.[14] Genotypically wild-type adult zebrafish were either the genotypically wild-type siblings of the *syu*$^{t4+/-}$ fish (Tuebingen [Tu] background strain) or of our outbred strain originally obtained from Scientific Hatcheries (SciH; Huntington Beach, CA). Fish were bred and raised at the University of Idaho according to Westerfield.[30] Fish were kept in monitored aquatic housing units (14 hours–10 hours light– dark cycle) employing filtered, recirculated water (28.5°C).

BrdU treatments were performed as published.[31,32] The fish were incubated in 5 mM BrdU in system water for 5 days with solutions changed on day 3. The fish were fed before the solution change. In these experiments, the fish were killed immediately after the 5-day BrdU treatment.

For the light-lesion experiments, 1.5-year postfertilization (pf) albino (*alb*) zebrafish were dark treated for 14 days and exposed to constant, intense light for 3 days, to cause rod and cone photoreceptor death in the dorsal retina.[26,33] To verify the light-induced photoreceptor damage and the initiation of retinal cell proliferation that characterizes the teleost retinal regeneration response, some fish were killed at the conclusion of the light treatment, and the eyes were processed for frozen section immunolocalization of rod opsin, blue cone opsin, and proliferating cell nuclear antigen (PCNA). [34] As expected, the immunolabeling demonstrated severe reductions in the rod and blue cone cells and a large number of PCNA^{+} cells within the inner and outer nuclear layers of the dorsal retina (data not shown). Both eyes from the remaining light-treated fish were used to examine the blue opsin gene expression pattern by wholemount retina in situ hybridizations. Thus, retinas from six fish were harvested after 3 days of light treatment, to assess the pattern of blue cone cell loss. In addition, six light-treated fish were returned to normal facility light conditions for 33 days and the retinas collected to assess the pattern of regenerated blue cone cells. Non–light-treated controls for this experiment included *alb* fish that were maintained in normal facility light conditions (three fish) and 14-day dark-treated *alb* fish that were returned to facility lighting (three fish).

Tissue Processing and Immunohistochemistry

Fish were anesthetized in buffered MS-222[30] and were killed by spinal cord transection. Subsequent to enucleations, lenses were removed through corneal perforations. The left eyes of each fish were processed for frozen section cell labeling, whereas the retinas were dissected from the right eyes of the fish for wholemount in situ RNA hybridizations. Dissected whole retinas were obtained from both eyes of fish from the light treatment experiment. Eyes processed for frozen section analysis were fixed in phosphate-buffered 4% paraformaldehyde-5% sucrose for 1 hour, washed in buffered 5% sucrose, and cryoprotected overnight in buffered 20% sucrose. The eyes were frozen embedded in a 2:1 solution of buffered 20% sucrose-OCT (Sakura Finetek, Torrance, CA) and cryosectioned at 3 to 5 μm. [35] For wholemount retinal analysis, dissected, fixed retinas were washed in buffered 5% sucrose and stored in 100% methanol at 4°C.

The following antibodies (and their dilutions) were used: rat monoclonal anti-BrdU (1:50; Accurate Chemical, Westbury, NY); mouse monoclonals zpr-1, zpr-3, and anti-HuC/D (all at 1:200; Zebrafish International Resource Center, University of Oregon); anti-glutamine synthetase (GS; 1:5000; BD Biosciences, San Diego, CA); anti-protein kinase C (PKC; 1:200; Santa Cruz Biotechnology, Santa Cruz, CA); and anti-PCNA (1:50; Biomeda Corp., Foster City, CA). Before primary antibody application, the sections for BrdU or PCNA detection were incubated in a 1:1 solution of 4 N HCl-PBS-0.05% Triton X-100 (PBST) for 30 minutes, followed by washes in PBST and PBS. In all cases, the sections were blocked in 20% normal goat serum and the primary antibodies were incubated overnight at 4°C. The sections were washed with PBST and incubated in the appropriate secondary antibody (Jackson ImmunoResearch, West Grove, PA) for 2 hours at room temperature. The immunolabeled sections were washed in PBST, and coverslips were mounted (Vectashield; Vector Laboratories, Burlingame, CA).

Tissue In Situ RNA Hybridization

Hybridization was performed as previously described.[36] Digoxigenin-labeled (DIG) cRNA probes were prepared from full-length cDNAs corresponding to blue cone and rod opsin using components of the Genius Kit (Roche, Indianapolis, IN). Cryosections were hydrated through an ethanol series before incubation with 1 mg/mL proteinase K at 37°C for 2 minutes (sections) or 30 minutes (whole retinas). Tissues were treated with acetic anhydride in triethanolamine buffer for 10 minutes, dehydrated, and hybridized with 4 mg/mL DIG probe in a hybridization buffer containing 50% formamide overnight at 65°C. Hybridization was detected with an anti-DIG antibody conjugated to alkaline phosphatase and the color substrates 4-nitroblue tetrazolium chloride and 5-bromo-4-chloro-3-indolyl phosphate (NBT/BCIP).

Cell Death Detection

Detection of cell death was performed using an in situ cell death detection kit based on the terminal dUTP nick-end labeling (TUNEL) method (Roche) according to the manufacturer's instructions. Incorporated fluorescein-tagged dUTPs were amplified using peroxidase-conjugated anti-fluorescein followed by a diaminobenzidine color reaction.[13] Endogenous peroxidases were quenched before the TUNEL procedure by incubating slides in 0.3% H_2O_2.

Microscopy, Imaging, and Pattern Analysis

Sections were viewed on an epifluorescence microscope (DMR; Leica, Deerfield, IL) and/or bright-field or Nomarski optics. Images were collected with a digital camera (Spot; Diagnostic Instruments, Sterling Heights, MI) and associated software. Each section was imaged in its entirety to enable visual inspection of the entire retina for any photoreceptor abnormalities. In the BrdU-exposed animals, the total number of $BrdU^+$ cells in each retinal layer was counted for each section, and the individual section counts were averaged for each fish.

Images of wholemounted retinas processed for blue cone opsin in situ hybridization were used for spatial pattern analysis. In the light-treated *alb* retinas, we evaluated the dorsal retina, but did not include the ventral retina in our analysis because minimal light-induced in this retinal region fails to stimulate a significant regenerative response.[33] This lack of response was evident in the light-treated eyes because the ventral retinas retained the precise blue cone mosaic pattern. We randomly selected 3 to 10 optically coplanar, 110 × 110 μm regions that were free of folds, wrinkles, or tears, for quantitative pattern analysis. These images were imported into ImageJ (available by ftp at zippy.nimh.nih.gov/ or at http://rsb.info.nih.gov/nih-image; developed by Wayne Rasband, National Institutes of Health, Bethesda, MD) for assignment of unique *x,y* coordinates corresponding to the labeled blue cones. The *x,y* coordinates were subjected to two methods of spatial pattern analysis using

custom-made software[36,37]: nearest neighbor distance analysis (NND)[32]; and quadrat analysis.[36,38] After NND analysis, conformity ratios (CRs) were calculated as the mean NND/SD; CRs were used to determine whether a particular pattern was significantly different from a random pattern.[39] Quadrat analysis involved the calculation of a statistical measure (var/mean)($N - 1$), which allows for the assignment of pattern attributes as significantly more regular, or more aggregated than those expected for a Poisson distribution.[36] Statistical comparisons of proportions of retinal regions having specific assigned pattern attributes were performed using the nonparametric Kolmogorov-Smirnov test. Statistical comparisons of planimetric densities were performed by using one-way ANOVA followed by a Fisher's post hoc least significant differences test.

RT-PCR and Quantitative RT-PCR

Wild-type ($n = 3$) and *syu*$^{+/-}$ ($n = 3$) zebrafish were anesthetized and killed by spinal cord transection, and the retinas were harvested for RNA extraction. Tissue was homogenized, and RNA extraction was performed (RNeasy Mini Kit; Qiagen, Valencia, CA) followed by oncolumn DNase treatment. The quantity of RNA was determined spectrophotometrically by the A260/A280 ratio (Nanodrop 1000; Thermo-Scientific, Wilmington, DE).

RNA from adult wild-type and *syu*$^{+/-}$ zebrafish retinas was amplified by semiquantitative RT-PCR (One-Step kit; Qiagen). Samples were amplified using the following conditions: 5 minutes at 94°C, 40 cycles of 45 seconds at 94°C, 45 seconds at 58°C, 2 minutes at 72°C. The following primers were used: *β*-actin, 5′-TGGTATTGTGATGGACTCTGG (forward) and 5′-AGCACTGTGTTGGCATACAGG (reverse) resulting in a 450-bp product[40]; *ptc-2*, 5′-CTACAGCCCTCCACCCTCCTAC (forward) and 5′-CGTATACCAGAATCCCCAAACTGAG (reverse) resulting in a 333-bp product[7]; and *shh* 5′-CCACTACGAGGGAAGAGCTG (forward) and 5′-GCTGACCGCTATCATCAACA (reverse) resulting in a 500-bp product, designed using the Web-based application, Primer 3.[41]

Expression levels of *shh* mRNA in wild-type and *syu*$^{+/-}$ zebrafish retinas were quantified by quantitative real-time RT-PCR (qRT-PCR). For each sample, first-strand cDNA was synthesized with 100 ng of total RNA, 100 ng random primers (Invitrogen, Carlsbad, CA), and 50 U reverse transcriptase (Superscript II; Invitrogen), according to the manufacturer's protocol. DNase I (Fermentas, Glen Burnie, MD) was used to remove possible DNA contamination. qRT-PCR was performed (model 7900HT Fast Real-Time PCR System using SYBR-Green PCR Master Mix; Applied Biosystems, Inc. [ABI], Foster City, CA) according to the manufacturer's protocol. cDNAs were diluted 1:5 with TE (pH 8.0) and used as a template in the reactions. Specificity of the reactions was verified with melting-curve analysis. Three biological replicates and two technical replicates were performed for each tissue type. 18S rRNA was used as the endogenous reference gene.[34] Before statistical analysis, C_T values for both the target genes and the reference gene were averaged across technical replicates. The target gene was then normalized to the endogenous control, and an unpaired *t*-test was used to test for differences in *shh* expression between wild-type and *syu*$^{+/-}$ tissues.

Results

Regional Cone Loss and Morphologic Abnormalities in the Retinas of Senescent *syu*$^{t4+/-}$ Zebrafish

The organization and morphology of double cone photoreceptors in wild-type and *syu* heterozygotes (*syu*$^{+/-}$) were analyzed by indirect immunofluorescence of retinal frozen sections using the zpr-1 antibody, which labels a surface epitope on both the red-and green-sensitive cones of the zebrafish retina.[42] In young (3–10 months pf) wild-type fish, the zpr-1

immunofluorescence revealed the double cone synaptic terminals, axons, cell bodies, and inner and outer segments (Fig. 1; Table 1). The young *syu*$^{+/-}$ fish also displayed a normal double-cone–labeling pattern with the double cone cell morphology displaying laminar positioning that was identical with that in the wild-type. Similarly, the double cones of older (1.5 years pf), though not reproductively senescent, *syu*$^{+/-}$ fish also appeared similar to those in the wild-type (Fig. 1; Table 1). The retinas from reproductively senescent (2 years and older) wild-type fish also displayed no detectable abnormalities in the double-cone arrangement or morphology based on the frozen section immunolabeling (Fig. 1; Table 1). However, half of the retinas (n = 12) derived from 2 years pf *syu*$^{t4+/-}$ fish contained regions of double-cone loss and abnormalities including a lack of outer segments. In some cases these regions of cone abnormality were adjacent to retinal regions that were characterized by increased cone density (Fig. 1F). Retinas derived from *syu*$^{tbx+/-}$ fish did not display these overt abnormalities, although some retinas possessed regions of reduced zpr-1^{+} cone density (Table 1, and data not shown). This cone loss phenotype was therefore both age- and genotype-specific.

To confirm the regional cone loss and cone morphologic abnormalities exhibited by the 2-year-old *syu*$^{+/-}$ fish were not restricted to the double-cone cell population, and to evaluate cone loss across entire retinas, we examined the long single-cone (blue cones) organization by wholemount in situ RNA hybridization. Retinas were obtained from young, middle-aged, and old (<10 months pf, 1.5 years pf, and >2 years pf, respectively) wild-type and *syu*$^{t4+/-}$ zebrafish, processed for in situ hybridization with a blue opsin cRNA probe and flat-mounted for imaging the long single-cone population. Retinas of wild-type fish of all ages and the youngest *syu*$^{t4+/-}$ fish displayed a geometrically precise blue cone mosaic (Figs. 2A-D; Table 1). Likewise, the middle-aged *syu*$^{t4+/-}$ fish displayed a precise cone mosaic, although in a few cases a small number of cones were missing from the mosaic (Fig. 2E; Table 1) or appeared structurally irregular (not shown). In marked contrast, all retinas obtained from the oldest *syu*$^{t4+/-}$ fish exhibited a highly irregular blue cone pattern with regions of low cone density alternating with regions of higher density (Fig. 2F; Table 1). Unusual patterns similar to those of middle-aged *syu*$^{t4+/-}$ fish were also regularly observed in retinas obtained from old *syu*$^{tbx+/-}$ zebrafish (Fig. 2G; Table 1).

To determine whether the retinal abnormalities in aging *syu*$^{t4+/-}$ zebrafish were cone-specific, several retinal cell type-specific markers were examined by immunolabeling retinal cryosections from wild-type and *syu*$^{t4+/-}$ zebrafish at 1.5 and 2+ years pf. Zpr-3, a monoclonal antibody selective for rod opsin, labeled rod outer segments in all fish examined including the oldest *syu*$^{+/-}$ fish (Figs. 3A-D; n = 3 for each genotype/age, average of 18 sections examined per eye). In the zpr-3-labeled sections, there were no indications of rod outer segment loss or damage, even in regions exhibiting cone abnormalities. Tissue in situ hybridizations of retinal sections using a rod opsin cRNA probe were also performed to assess further the potential abnormalities in the rod photoreceptors. This test failed to reveal any unusual rod cell labeling patterns or morphologies (data not shown). Sections were also immunolabeled by using antibodies to detect protein kinase C (PKC, rod bipolar cells; Figs. 3E-H), HuC/D (ganglion and amacrine cells; Figs. 3I-L), and glutamine synthetase (GS, Müller glia; Figs. 3M-P). In all cases, the labeling patterns in the *syu*$^{+/-}$ retinas appeared equivalent to wild-type (n = 3–7 for each genotype/age, average of 18, 28, and 40 sections examined per eye for PKC, HuC/D, and GS, respectively). Thus, the rod photoreceptors, amacrine, and ganglion cells, as well as the rod bipolar and Müller glia in the aged *syu*$^{+/-}$ retinas appeared normal in terms of organization and cellular morphology. These data indicate the *syu*$^{+/-}$ retinal phenotype is cone-specific.

Cone Patterns in Aging *syu*$^{t4+/-}$ Retinas and in Retinas Subjected to Acute Photoreceptor Damage

The geometrically precise cone cell pattern of teleost retinas becomes disrupted after light-induced photoreceptor damage[26] and is statistically distinct from the undamaged, wild-type condition after retinal regeneration.[36] To gain additional insights into the cone loss phenotype in aging *syu*$^{t4+/-}$ retinas, we compared the *syu* heterozygote cone pattern with the cone pattern in a model of acute cone cell loss and regeneration caused by light-induced.[26] Whole retinas were obtained from *alb* zebrafish subjected to 3 days of constant, intense light or from light-treated *alb* fish after a 33-day period of regeneration. These retinas were processed for wholemount in situ hybridizations using a blue cone opsin cRNA probe and flatmounted for imaging and analysis. Qualitatively, the blue cone patterns of all non–light-treated control *alb* fish displayed the geometrically precise cone mosaic (Fig. 4A). In contrast, the blue cone pattern in the dorsal retinal regions of the light-treated *alb* zebrafish was sparse and irregular (Fig. 4B). The *alb* regenerated retinas also displayed an irregular blue cone pattern, but the cells were more densely arranged than in the retinas at the conclusion of the light treatment (Fig. 4C).

Images such as those in Figures 2 and 4 were used to identify unique *x,y* coordinates of labeled cells, and the resultant cone distributions were quantitatively evaluated with NND and quadrat analyses.[36,39] The application of NND analysis, which emphasizes local patterning attributes, to the blue cone pattern revealed predominantly statistically regular patterns in all wild-type retinas and in all untreated control *alb* retinas, with a normal distribution of NND values and a correspondingly high conformity ratio (Fig. 5A, top histograms). In many regions of the 1.5 years pf *syu*$^{t4+/-}$ retinas, and in most regions of the oldest *syu*$^{t4+/-}$ retinas, blue cones showed a progressively less normal distribution, and conformity ratios indicating a pattern not significantly different from random (Fig. 5A, middle histogram). Similarly, the blue cone patterns of the light-damaged *alb* dorsal retina showed statistically random patterns of blue cones (Fig. 5A, bottom right histogram). In the regenerated dorsal retinas of the light-treated *alb* zebrafish, NND analysis again showed statistically random patterns of blue cones (Fig. 5A, bottom left). These analyses suggest that local blue cone pattern abnormalities associated with *syu*$^{t4+/-}$ and light-induced damage were statistically similar.

The application of quadrat analysis to the blue cone organization allowed quantitative evaluation of global pattern attributes, including regularity and aggregation ("clumping"[36, 38]). All the patterns categorized as "regular" by NND analysis were also found by quadrat analysis to be regular (Fig. 5B). Blue cone patterns in middle-aged (1.5 years) *syu*$^{t4+/-}$ retinas were characterized by quadrat analysis as not significantly different from random. Similarly, blue cone patterns of *alb* retinas obtained immediately after light-induced damage were also random (Fig. 5B). However, in some regions of the *syu*$^{t4+/-}$ retinas and in some regions of the *alb* retinas allowed to regenerate after light treatment, quadrat analysis indicated statistically clumped patterns (Fig. 5B). Collectively, these data suggest quantitative similarities in the blue cone pattern of *syu*$^{t4+/-}$ retinas and the retinas subjected to photoreceptor-specific damage. The pattern changes, however, were not uniform across all regions within a retina, nor between individual fish.

Figure 6 summarizes the pattern trends for the analyzed ages, genotypes, and treatments. NND analysis revealed consistently regular patterns in wild-type animals, an increasing tendency toward random patterns with age in *syu*$^{t4+/-}$ and *syu*$^{tbx+/-}$ retinas, and predominantly random patterns in the dorsal retinas of *alb* zebrafish subjected to light toxicity, both before and after a period of regeneration (Fig. 6A). The shift from predominantly regular to random patterns was statistically significant ($P < 0.05$) between young and old *syu*$^{+/-}$ retinas of both genotypes and between any two of the three conditions for the *alb* retinas. Quadrat analysis revealed consistently regular patterns in wild-type animals, tendencies toward both randomness and

clumping in *syu*$^{t4+/-}$ and the regenerated dorsal *alb* retinas, and tendencies toward randomness in the dorsal *alb* retinas immediately after acute light toxicity (Fig. 6B). The reduction in proportions of the analyzed regions showing long-range regularity was statistically significant ($P < 0.05$) between any two of the four conditions for the *syu*$^{+/-}$ retinas, and between control and light-treated *alb* retinas. The increase in proportions of analyzed regions showing blue cone clumping was statistically significant ($P < 0.05$) between young and old *syu*$^{t4+/-}$ retinas and between regenerated and nonregenerated *alb* retinas. Planimetric density of blue cones did not change significantly with age in either wild-type or *syu*$^{t4+/-}$ retinas (Fig. 6C). The density of blue cones decreased significantly however, compared with the control after light-induced damage ($P < 0.05$) and then increased significantly after regeneration ($P < 0.05$; Fig. 6C). These results are consistent with a regenerative response that has not fully resolved the native local or global pattern of blue cones.

Retinal Cell Death and Proliferation

To determine whether and when cone photoreceptors die, we processed retinal sections from wild-type and *syu*$^{t4+/-}$ zebrafish at 1.5 and 2+ years pf for TUNEL. We used sectioned *syu*$^{t4-/-}$ embryos as positive controls (not shown), as their retinal tissue invariably displays widespread cell death.[13] TUNEL$^+$ cells were rarely observed in any of the adult retinal sections (data not shown), and the number of TUNEL$^+$ cells in *syu*$^{t4+/-}$ retinas was not significantly different from that in the wild-type retinas (Table 2).

The zebrafish retina is capable of robust retinal cell regeneration after both widespread and cell-selective injuries.[22,27] The regenerated cells arise from a proliferative population of inner nuclear layer cells, at least some of which correspond to Müller glia.[34,43-45] To determine whether the *syu*$^{t4+/-}$ retinal cone cell loss was stimulating a cone regeneration response as indicated by increased retinal cell divisions, we treated age-matched wild-type and *syu*$^{+/-}$ zebrafish systemically with 5 mM BrdU for 5 days and obtained retinal sections to assess BrdU incorporation. In rare cases, we observed BrdU$^+$ cells within the ONL and the outer half of the INL (Fig. 7; Table 2). However, the number of BrdU$^+$ cells in *syu*$^{t4+/-}$ retinas was not significantly different from that of wild-type retinas (Table 2). Experiments using an antibody to detect PCNA, an independent indicator of cell cycle progression[32] similarly revealed no significant proliferative activity in the *syu*$^{t4+/-}$ retinas (data not shown). Taken together, the TUNEL, BrdU incorporation, and PCNA immunohistochemistry suggest that the cell death and cell proliferation responses in the *syu*$^{+/-}$ retinas must occur at very low levels over a prolonged time course.

Expression of Sonic Hedgehog and Patched2 mRNA

To determine whether *shh* expression and signaling were reduced in the *syu*$^{t4+/-}$ fish compared with wild-type, we performed semiquantitative RT-PCR using specific primers for *shh* and *patched-2 (ptc2*) on RNA obtained from isolated retinas. Expression of *Patched* genes is positively regulated by Shh signaling,[46] and *ptc2* expression has been demonstrated in the embryonic zebrafish retina.[7] PCR products of the appropriate size were consistently amplified from 10, 5, and 2.5 ng of total RNA. Isolated retinas from *syu*$^{+/-}$ fish contained lower quantities of both *shh* and *ptc2* mRNA (Fig. 8A). qRT-PCR analysis confirmed these findings for *shh* expression, with significant difference between *shh* expression in the retina of wild-type versus *syu*$^{+/-}$ ($P = 0.0265$; Fig. 8B). Mean normalized ΔC_T values for wild-type and *syu*$^{+/-}$ retina were 19.68187 and 20.73061, respectively.

Discussion

Age-Related, Cone-Restricted Phenotype in the *syu*$^{+/-}$ Zebrafish Retina

This study revealed an age-related detrimental effect of heterozygosity at the *syu* locus that specifically affects cone photoreceptors. In young adult *syu*$^{+/-}$ zebrafish and in all ages of wild-type fish examined, cone photoreceptors displayed normal morphology and a regular mosaic distribution. In contrast, the oldest *syu*$^{+/-}$ zebrafish displayed retinal regions characterized by missing cones, clumped cones, or cones with abnormal morphology. This phenotype was clearly associated with the *syu*$^{+/-}$ genotype and was more pronounced in carriers of the *shh* deletion (*syu*^{t4}) than in those of the point mutation (*syu*^{tbx}). Rod photoreceptors and other retinal cell types were unaffected, based on immunolocalizations and in situ hybridizations to detect various retinal cell-type markers. Although the *syu*$^{t4+/-}$ blue cone pattern phenotype exhibits incomplete penetrance in middle-aged fish (1.5 years), it is fully penetrant in old, reproductively senescent individuals. At this stage of the zebrafish lifespan, retinal growth is negligible,[47] indicating the cone degeneration occurred within extant retina. This constitutes the first report in zebrafish of retinal abnormalities associated with postreproductive senescence.

Statistical comparisons of the cone patterns in aged *syu*$^{+/-}$ retinas and light-damaged retinas demonstrated the perturbations in *syu*$^{+/-}$ cone pattern are consistent with cone loss followed by, or accompanied by, a cone regeneration response (see also Refs. 26,[36]). However, the changes in the *syu*$^{+/-}$ cone pattern were not accompanied by detectable alterations in cell death or cell proliferation. This result may be expected for several reasons. The cone abnormalities in the *syu*$^{t4+/-}$ retinas did not become evident until late adulthood. This phenotype indicates the cone disease develops over an protracted time course. Our sampling of single time points during this extended period would be expected to miss relatively infrequent cone cell death events. These low levels of photoreceptor cell death may not be adequate to stimulate the high levels of cell proliferation previously observed in zebrafish models of retinal cell regeneration, in which widespread cell death was induced by treatment with intense light or acute trauma.[26,32,36,44,45] Regenerative cell proliferation may also be influenced by the mitogenic function of Shh[5,10,13,48]; reduction of Shh in the *syu*$^{+/-}$ retinas may limit the extent of the retinal cell proliferation response. The requirement for supplemental Shh in the regenerating embryonic chick retina supports this hypothesis.[49]

Sonic Hedgehog for Adult Cone Maintenance and Survival

Our results suggest Shh activity is necessary for the maintenance and survival of the cone photoreceptor cells in the adult retina. During retinal development, *shh* is expressed in ganglion cells, amacrine cells,[3,6] and the RPE.[7-9] Experimental reductions in Shh signaling resulted in reduced retinal progenitor proliferation,[13] a reduction in differentiated ganglion cells[4] and photoreceptors,[7,12,13] and RPE defects.[8] We report here that expression of *shh* persists in the adult, wild-type zebrafish retina, but *shh* mRNA is significantly reduced in the retinas of the *syu*$^{t4+/-}$ fish. Our semiquantitative RT-PCR results suggest further that Shh signaling activity is also reduced within the retina so that expression of the target gene *ptc2* is affected. The age-related cone abnormalities are therefore associated with reduced *shh* expression and signaling in the retina. Cone photoreceptors may require some threshold amount of Shh throughout the zebrafish lifespan, and this becomes limiting in the oldest *syu*$^{+/-}$ fish. An analysis of Shh-related gene expression—including that of *twhh*— in isolated retina and RPE tissue will address the question of whether hedgehog gene expression and signaling is also affected in the RPE of adult, aging *syu*$^{+/-}$ fish.[7]

Mutations in Shh or in the molecular components of its signal transduction pathway have not been directly associated with any human retinal disorder or any other animal model of retinal

disease. However, major risk factors for human age-related macular degeneration (AMD) include metabolic errors in cholesterol homeostasis.[50] In addition, cholesterol deficiency or elevated sterol precursors cause profound congenital abnormalities, including ocular defects[51] and retinal degeneration.[52] The Shh signal transduction pathway requires cholesterol, and Shh signaling can be altered by sterols.[53] Thus, proper regulation of cholesterol homeostasis and Shh signaling may be necessary to maintain photoreceptor health in the human retina.

The age-related cone abnormality phenotype was less pronounced in carriers of the *tbx* (point mutation) allele than in those of the *t4* (deletion) allele. Both alleles are considered null, and homozygous mutants exhibit nearly identical embryonic phenotypes.[14] The retinal phenotype associated with heterozygosity may have uncovered incomplete penetrance of the *tbx* allele. Alternatively, the more severe $syu^{t4+/-}$ retinal phenotype may be due to the synergistic effect of the deletion on a nearby gene or gene regulatory elements. The deleted region of the syu^{t4} allele encompasses the entire *shh* coding region, along with 4.0 kb of 5′ sequence and 2.2 kb of 3′ sequence.[14] However, the nearest predicted open reading frame is located approximately 15.0 kb upstream of *shh*, based on a single expressed sequence tag (EST) identified from this genomic region. The expression of this gene may be affected by the syu^{t4} deletion through the loss of putative *cis*-regulatory elements. Characterization of carriers of other Hh pathway mutations is under way, to explore these possibilities. The $syu^{+/-}$ zebrafish nevertheless represents a genetically tractable model for investigating molecular determinants of human retinal dysgenesis and disease.

The $syu^{+/-}$ cone photoreceptors are disrupted in the absence of any overt impact on the rod photoreceptors, suggesting that the cone population is more sensitive to limiting levels of Shh signaling. Alternatively, the rod population may also be sensitive, but mechanisms for their continual addition may be compensating.[22,27] This cone-specific effect in the zebrafish $syu^{+/-}$ retinas is distinct from most human photoreceptor degenerations, including AMD, where rod photoreceptor death precedes cone cell death.[54-56] Mammalian models that mimic this sequence of photoreceptor loss were used to identify cone survival factors generated by rods that become limiting during rod degeneration.[57] However, other human retinal diseases are characterized by either the exclusive loss of cones, or the concurrent loss of both the cone and rod cells.[58,59] Similar to the aged $syu^{+/-}$ fish, larval-age *gnn* zebrafish mutants lose cones with little loss of rods.[60] In contrast, the *Xops*:mCFP transgene causes rod photoreceptor loss in zebrafish without detectable effects on the cone cell population.[61] Collectively, these zebrafish models confirm the variable degree of cone–rod interdependence and emphasize that non–cell-autonomous factors function to maintain cone viability and should be considered for their therapeutic potential.

Cone Patterning in Environmental and Genetic Models of Photoreceptor Damage

In zebrafish, retinal cells are regenerated in response to acute trauma or cellular insult that results in some threshold level of cell death.[22,27] The present study suggests that retinal regeneration is also stimulated in response to a genetic defect that results in cone photoreceptor degeneration. The cone regeneration response after photoreceptor-selective damage due to intense light treatment resulted in a disrupted cone mosaic that qualitatively and quantitatively resembled the disrupted cone mosaic after more widespread forms of retinal damage, such as whole-retina destruction with a toxin,[36] or surgical removal of a portion of retina.[20] This quantitatively predictable disruption in cone cell pattern was also observed in the aged $syu^{+/-}$ retinas. The fish retina may therefore incur a conserved cellular response to photoreceptor damage, resulting in densely clustered cones whose aberrant organization contributes to the surrounding region's cone loss phenotype. These findings also indicate that,

after photoreceptor damage, cone positional information contributed by the other retinal layers or remaining photoreceptors is not sufficient to restore the native cone mosaic pattern.

Acknowledgements

The authors thank Anand Chandrasekhar (University of Missouri); and Rolf Karlstrom (University of Massachusetts) for providing the *syu*$^{+/-}$ fish; Bhavani Kashyap, Savjit Singh, Jessica Thompson, and Rob Drew (University of Idaho) for technical assistance; and the University of Notre Dame Center for the use of the Zebrafish Research and the Freimann Life Sciences Center.

Supported by the American Health Assistance Foundation's Macular Degeneration Program (DLS), National Eye Institute Grant EY012146 (DLS), and National Science Foundation Grant 0351250 (DAC).

References

1. Stenkamp, DL. Multiple roles for hedgehog signaling in zebrafish eye development. In: Fisher, CE.; Howie, SEM., editors. Shh and Gli Signaling and Development. Landes Bioscience; Georgetown, TX: 2006. p. 58-68.
2. Wallace VA. Proliferative and cell fate effects of Hedgehog signaling in the vertebrate retina. Brain Res 2008;1192:61–75. [PubMed: 17655833]
3. Wallace VA, Raff MC. A role for Sonic hedgehog in axon-to-astrocyte signalling in the rodent optic nerve. Development 1999;126(13):2901–2909. [PubMed: 10357934]
4. Neumann CJ, Nuesslein-Volhard C. Patterning of the zebrafish retina by a wave of sonic hedgehog activity. Science 2000;289(5487):2137–2139. [PubMed: 11000118]
5. Zhang XM, Yang XJ. Regulation of retinal ganglion cell production by Sonic hedgehog. Development 2001;128(6):943–957. [PubMed: 11222148]
6. Shkumatava A, Fischer S, Müller F, Strahle U, Neumann CJ. Sonic hedgehog, secreted by amacrine cells, acts as a short-range signal to direct differentiation and lamination in the zebrafish retina. Development 2004;131(16):3849–3858. [PubMed: 15253932]
7. Stenkamp DL, Frey RA, Prabhudesai SN, Raymond PA. Function for Hedgehog genes in zebrafish retinal development. Dev Biol 2000;220(2):238–252. [PubMed: 10753513]
8. Perron M, Boy S, Amato MA, et al. A novel function for Hedgehog signalling in retinal pigment epithelium differentiation. Development 2003;130(8):1565–1577. [PubMed: 12620982]
9. Levine EM, Roelink H, Turner J, Reh TA. Sonic hedgehog promotes rod photoreceptor differentiation in mammalian retinal cells in vitro. J Neurosci 1997;17(16):6277–6288. [PubMed: 9236238]
10. Wan J, Zheng H, Xiao HL, She ZJ, Zhou GM. Sonic hedgehog promotes stem-cell potential of Muller glia in the mammalian retina. Biochem Biophys Res Commun 2007;363(2):347–354. [PubMed: 17880919]
11. Yu C, Mazerolle CJ, Thurig S, et al. Direct and indirect effects of hedgehog pathway activation in the mammalian retina. Mol Cell Neurosci 2006;32(3):274–282. [PubMed: 16815712]
12. Stenkamp DL, Frey RA. Extraretinal and retinal hedgehog signaling sequentially regulate retinal differentiation in zebrafish. Dev Biol 2003;258(2):349–363. [PubMed: 12798293]
13. Stenkamp DL, Frey RA, Mallory DE, Shupe EE. Embryonic retinal gene expression in sonic-you mutant zebrafish. Dev Dyn 2002;225(3):344–350. [PubMed: 12412019]
14. Schauerte HE, van Eeden FJ, Fricke C, Odenthal J, Strähle U, Haffter P. Sonic hedgehog is not required for the induction of medial floor plate cells in the zebrafish. Development 1998;125(15): 2983–2993. [PubMed: 9655820]
15. Szamier RB, Berson EL. Retinal ultrastructure in advanced retinitis pigmentosa. Invest Ophthalmol Vis Sci 1977;16(10):947–962. [PubMed: 908648]
16. Michaelides M, Hardcastle AJ, Hunt DM, Moore AT. Progressive cone and cone-rod dystrophies: phenotypes and underlying molecular genetic basis. Surv Ophthalmol 2006;51(3):232–258. [PubMed: 16644365]
17. Wang DY, Chan WM, Tam PO, et al. Gene mutations in retinitis pigmentosa and their clinical implications. Clin Chim Acta 2005;351(12):5–16. [PubMed: 15563868]

18. Dalke C, Graw J. Mouse mutants as models for congenital retinal disorders. Exp Eye Res 2005;81 (5):503–512. [PubMed: 16026784]
19. Raymond PA, Barthel LK, Rounsifer ME, Sullivan SA, Knight JK. Expression of rod and cone visual pigments in goldfish and zebrafish: a rhodopsin-like gene is expressed in cones. Neuron 1993;10(6): 1161–1174. [PubMed: 8318234]
20. Stenkamp DL, Cameron DA. Cellular pattern formation in the retina: retinal regeneration as a model system. Mol Vis 2002;8:280–293. [PubMed: 12181523]
21. Easter SS Jr, Malicki JJ. The zebrafish eye: developmental and genetic analysis. Results Probl Cell Differ 2002;40:346–370. [PubMed: 12353485]
22. Stenkamp DL. Neurogenesis in the fish retina. Int Rev Cytol 2007;259:173–224. [PubMed: 17425942]
23. Krock BL, Bilotta J, Perkins BD. Noncell-autonomous photoreceptor degeneration in a zebrafish model of choroideremia. Proc Natl Acad Sci U S A 2007;104(11):4600–4605. [PubMed: 17360570]
24. Keller ET, Murtha JM. The use of mature zebrafish (Danio rerio) as a model for human aging and disease. Comp Biochem Physiol C Toxicol Pharmacol 2004;138(3):335–341. [PubMed: 15533791]
25. Kishi S, Uchiyama J, Baughman AM, Goto T, Lin MC, Tsai SB. The zebrafish as a vertebrate model of functional aging and very gradual senescence. Exp Gerontol 2003;38(7):777–786. [PubMed: 12855287]
26. Vihtelic TS, Hyde DR. Light-induced rod and cone cell death and regeneration in the adult albino zebrafish (Danio rerio) retina. J Neurobiol 2000;44(3):289–307. [PubMed: 10942883]
27. Hitchcock P, Ochocinska M, Sieh A, Otteson D. Persistent and injury-induced neurogenesis in the vertebrate retina. Prog Retin Eye Res 2004;23(2):183–194. [PubMed: 15094130]
28. Maaswinkel H, Riesbeck LE, Riley ME, et al. Behavioral screening for nightblindness mutants in zebrafish reveals three new loci that cause dominant photoreceptor cell degeneration. Mech Ageing Dev 2005;126(10):1079–1089. [PubMed: 15922406]
29. Maaswinkel H, Mason B, Li L. ENU-induced late-onset night blindness associated with rod photoreceptor cell degeneration in zebrafish. Mech Ageing Dev 2003;124(1012):1065–1071. [PubMed: 14659595]
30. Westerfield, M. The Zebrafish Book: A Guide for the Laboratory Use of Zebrafish (Danio rerio). 4. Eugene, OR: University of Oregon Press; 2000.
31. Otteson DC, D'Costa AR, Hitchcock PF. Putative stem cells and the lineage of rod photoreceptors in the mature retina of the goldfish. Dev Biol 2001;232(1):62–76. [PubMed: 11254348]
32. Sherpa T, Fimbel SM, Mallory DE, et al. Ganglion cell regeneration following whole-retina destruction in zebrafish. Dev Neurobiol 2008;68:166–181. [PubMed: 18000816]
33. Vihtelic TS, Soverly JE, Kassen SC, Hyde DR. Retinal regional differences in photoreceptor cell death and regeneration in light-lesioned albino zebrafish. Exp Eye Res 2006;82(4):558–575. [PubMed: 16199033]
34. Kassen SC, Ramanan V, Montgomery JE, et al. Time course analysis of gene expression during light-induced photoreceptor cell death and regeneration in albino zebrafish. Dev Neurobiol 2007;67(8): 1009–1031. [PubMed: 17565703]
35. Barthel LK, Raymond PA. Improved method for obtaining 3-microns cryosections for immunocytochemistry. J Histochem Cytochem 1990;38(9):1383–1388. [PubMed: 2201738]
36. Stenkamp DL, Powers MK, Carney LH, Cameron DA. Evidence for two distinct mechanisms of neurogenesis and cellular pattern formation in regenerated goldfish retinas. J Comp Neurol 2001;431 (4):363–381. [PubMed: 11223808]
37. Cameron DA, Carney LH. Cell mosaic patterns in the native and regenerated inner retina of zebrafish: implications for retinal assembly. J Comp Neurol 2000;416(3):356–367. [PubMed: 10602094]
38. Grieg-Smith, P. Quantitative Plant Ecology. 2. London: Butterworth; 1964.
39. Cook JE. Spatial properties of retinal mosaics: an empirical evaluation of some existing measures. Vis Neurosci 1996;13(1):15–30. [PubMed: 8730986]
40. DeCarvalho AC, Cappendijk SL, Fadool JM. Developmental expression of the POU domain transcription factor Brn-3b (Pou4f2) in the lateral line and visual system of zebrafish. Dev Dyn 2004;229(4):869–876. [PubMed: 15042710]

41. Rozen S, Skaletsky H. Primer3 on the WWW for general users and for biologist programmers. Methods Mol Biol 2000;132:365–386. [PubMed: 10547847]
42. Larison KD, Bremiller R. Early onset of phenotype and cell patterning in the embryonic zebrafish retina. Development 1990;109(3):567–576. [PubMed: 2401210]
43. Fimbel SM, Montgomery JE, Burket CT, Hyde DR. Regeneration of inner retinal neurons after intravitreal injection of ouabain in zebrafish. J Neurosci 2007;27(7):1712–24. [PubMed: 17301179]
44. Fausett BV, Goldman D. A role for alpha1 tubulin-expressing Muller glia in regeneration of the injured zebrafish retina. J Neurosci 2006;26(23):6303–6313. [PubMed: 16763038]
45. Yurco P, Cameron DA. Responses of Muller glia to retinal injury in adult zebrafish. Vision Res 2005;45(8):991–1002. [PubMed: 15695184]
46. Concordet JP, Lewis KE, Moore JW, et al. Spatial regulation of a zebrafish patched homologue reflects the roles of sonic hedgehog and protein kinase A in neural tube and somite patterning. Development 1996;122(9):2835–2846. [PubMed: 8787757]
47. Marcus RC, Delaney CL, Easter SS Jr. Neurogenesis in the visual system of embryonic and adult zebrafish (Danio rerio). Vis Neurosci 1999;16(3):417–424. [PubMed: 10349963]
48. Moshiri A, McGuire CR, Reh TA. Sonic hedgehog regulates proliferation of the retinal ciliary marginal zone in posthatch chicks. Dev Dyn 2005;233(1):66–75. [PubMed: 15759272]
49. Spence JR, Madhavan M, Ewing JD, et al. The hedgehog pathway is a modulator of retina regeneration. Development 2004;131(18):4607–4621. [PubMed: 15342484]
50. Chamberlain M, Baird P, Dirani M, Guymer R. Unraveling a complex genetic disease: age-related macular degeneration. Surv Ophthalmol 2006;51(6):576–586. [PubMed: 17134647]
51. Javitt NB. Oxysterols: functional significance in fetal development and the maintenance of normal retinal function. Curr Opin Lipidol 2007;18(3):283–288. [PubMed: 17495602]
52. Fliesler SJ, Peachey NS, Richards MJ, Nagel BA, Vaughan DK. Retinal degeneration in a rodent model of Smith-Lemli-Opitz syndrome: electrophysiologic, biochemical, and morphologic features. Arch Ophthalmol 2004;122(8):1190–1200. [PubMed: 15302661]
53. Cohen MM Jr. The hedgehog signaling network. Am J Med Genet A 2003;123(1):5–28. [PubMed: 14556242]
54. Curcio CA. Photoreceptor topography in ageing and age-related maculopathy. Eye 2001;15:376–383. [PubMed: 11450761]
55. Reme CE, Grimm C, Hafezi F, Iseli HP, Wenzel A. Why study rod cell death in retinal degenerations and how? Doc Ophthalmol 2003;106(1):25–29. [PubMed: 12675482]
56. Chader GJ. Animal models in research on retinal degenerations: past progress and future hope. Vision Res 2002;42(4):393–399. [PubMed: 11853755]
57. Leveillard T, Mohand-Saïd S, Lorentz O, et al. Identification and characterization of rod-derived cone viability factor. Nat Genet 2004;36(7):755–759. [PubMed: 15220920]
58. Michaelides M, Hunt DM, Moore AT. The cone dysfunction syndromes. Br J Ophthalmol 2004;88 (2):291–297. [PubMed: 14736794]
59. Simunovic MP, Moore AT. The cone dystrophies. Eye 1998;12:553–565. [PubMed: 9775217]
60. Biehlmaier O, Neuhauss SC, Kohler K. Double cone dystrophy and RPE degeneration in the retina of the zebrafish *gnn* mutant. Invest Ophthalmol Vis Sci 2003;44(3):1287–1298. [PubMed: 12601061]
61. Morris AC, Schroeter EH, Bilotta J, Wong RO, Fadool JM. Cone survival despite rod degeneration in XOPS-mCFP transgenic zebrafish. Invest Ophthalmol Vis Sci 2005;46(12):4762–4771. [PubMed: 16303977]

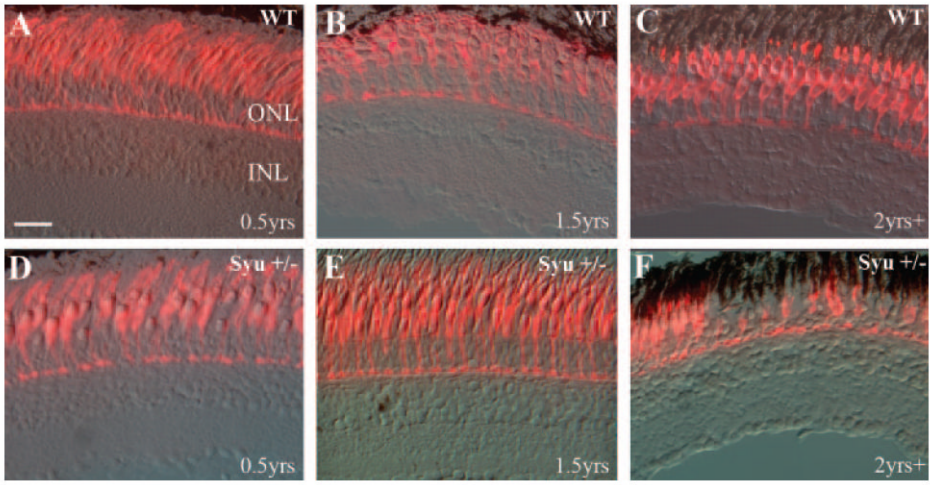

Figure 1.

Double-cone photoreceptor abnormalities in aging *syu*$^{+/-}$ zebrafish. Retinal cryosections from young (3–10 months pf; **A**, **D**), middle-aged (1.5 years pf; **B**, **E**), and reproductively senescent (2 years plus; **C**, **F**) wild-type (**A**–**C**) and *syu*$^{t4+/-}$ (**D**–**F**) zebrafish were immunolabeled with the monoclonal antibody zpr-1 to visualize the double-cone cells. Zpr-1^{+} cones were abundant and regularly spaced in all wild-type retinas (**A**–**C**) and the youngest and middle-aged *syu*$^{t4+/-}$ retinas (**D**, **E**). Sections from the oldest *syu*$^{t4+/-}$ fish, however, demonstrated sporadic loss and dysmorphism of the double-cone photoreceptors (**F**). ONL, outer nuclear layer; INL, inner nuclear layer. Scale bar, 25 μm.

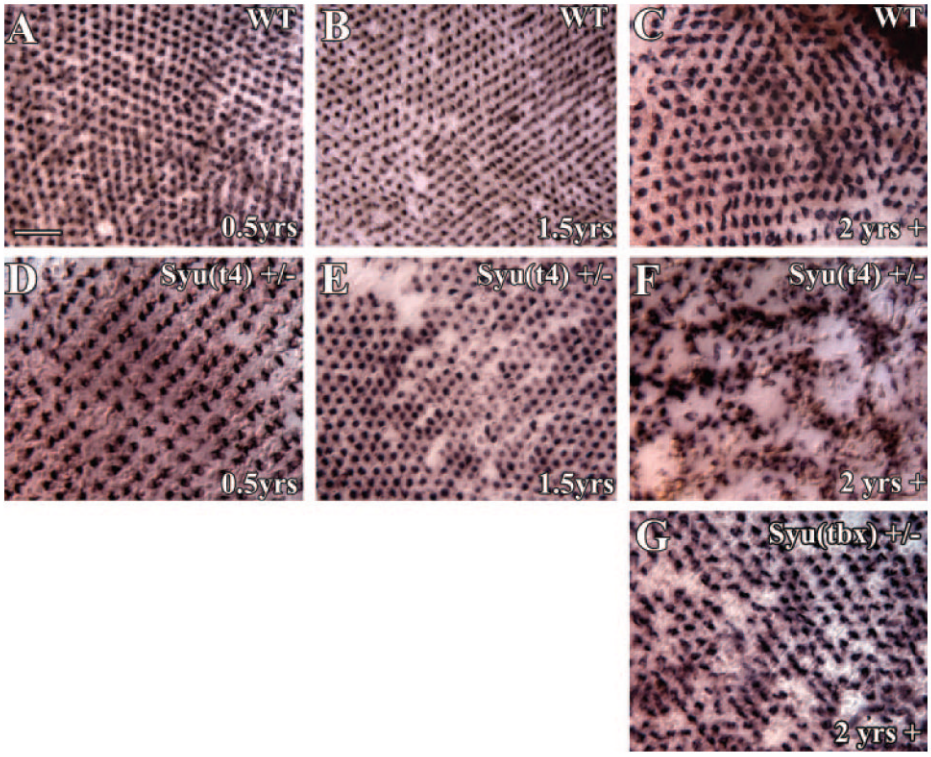

Figure 2.

Age-dependent loss and maldistribution of blue cones in aging *syu*$^{+/-}$ zebrafish. Retinal whole-mounts from young (3–10 months pf; **A**, **D**), middle-aged (1.5 years pf; **B**, **E**), and old (2 years plus; **C**, **F**) wild-type (**A**–**C**) and *syu*$^{t4+/-}$ (**D**–**F**) zebrafish were hybridized in situ with a blue opsin cRNA probe to identify the blue cones specifically. A precise blue cone mosaic was present in the wild-type retinas (**A**–**C**) and the youngest *syu*$^{t4+/-}$ retinas (**D**). A few retinas from middle-aged *syu*$^{t4+/-}$ fish were missing blue cones (**E**), whereas at least half of the oldest *syu*$^{t4+/-}$ retinas were characterized by large regions lacking this cone photoreceptor type (**F**). Notice the blue cone-deficient regions are surrounding clusters of very densely spaced blue opsin-positive cells. (**G**) A disrupted blue cone mosaic, reminiscent of that observed in middle-aged *syu*$^{t4+/-}$ fish, is evident in old *syu*$^{tbx+/-}$ (see also Fig. 6). Scale bar, 25 μm.

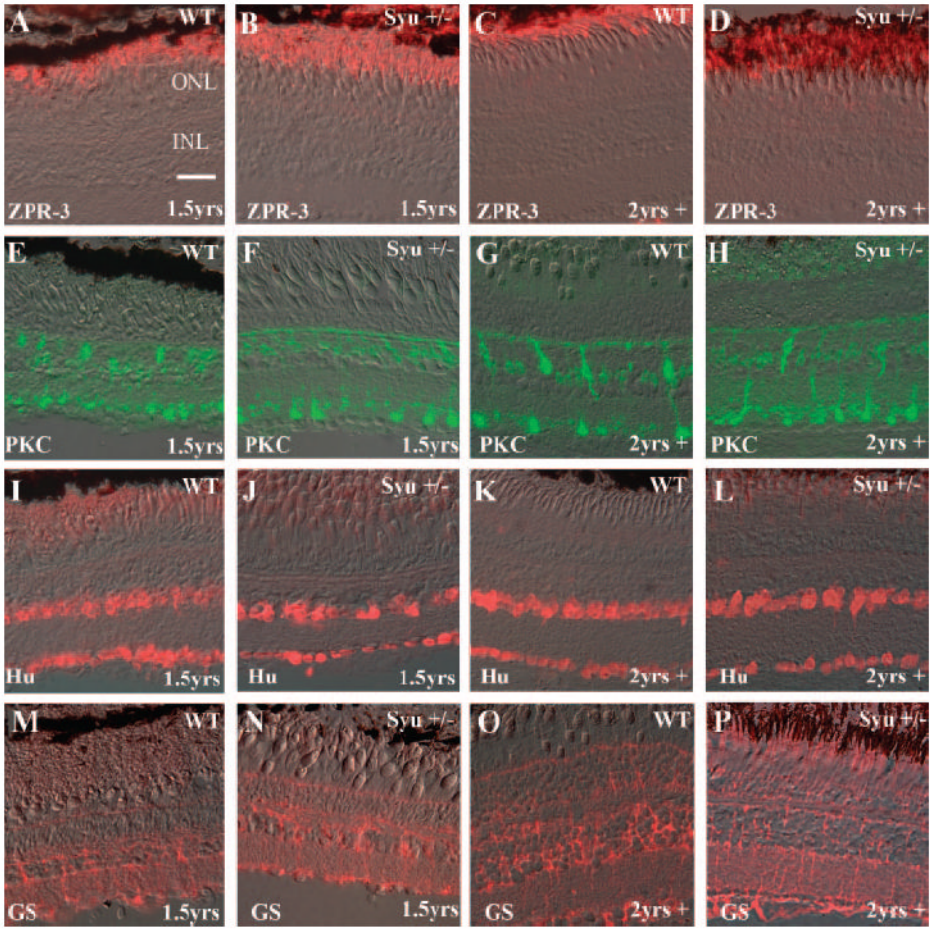

Figure 3.

Retinal cell-type analysis demonstrates that the cellular defects in the *syu*$^{t4+/-}$ retinas were cone-specific. Retina cell-type-specific markers were immunolocalized in eye frozen sections from aging wild-type and *syu*$^{+/-}$ fish. (**A**–**D**) The monoclonal antibody zpr-3 labeled rhodopsin in the rod outer segments. The rod photoreceptor number and morphology in the middle-aged (1.5 years; **B**) and older (2 years plus; **D**) *syu*$^{t4+/-}$ retinas were equivalent to wild-type (**A**, **C**). Anti- PKC labeled the cell bodies and processes of the rod bipolar cells. Anti-PKC immunolabeling demonstrated rod bipolar cells in the retinas of the middle-aged (**F**) and older *syu*$^{t4+/-}$ (**H**) fish were equivalent to the wild-type control (**E**, **G**). Amacrine and ganglion cells were identified by HuC/D protein expression. Retinal cryosections from middle-aged (**I**, **J**) and older (**K**, **L**) wild-type (**I**, **K**) and *syu*$^{t4+/-}$ (**J**, **L**) zebrafish possessed an equivalent number of amacrine and ganglion cells with wild-type morphology and organization. The glutamine synthetase (GS) protein expression pattern, which characterizes the Müller glia was also equivalent in the middle-aged (**M**, **N**) and reproductively senescent (**O**, **P**) wild-type (**M**, **O**) and *syu*$^{t4+/-}$ (**N**, **P**) zebrafish. ONL, outer nuclear layer; INL, inner nuclear layer. Scale bar, 25 μm.

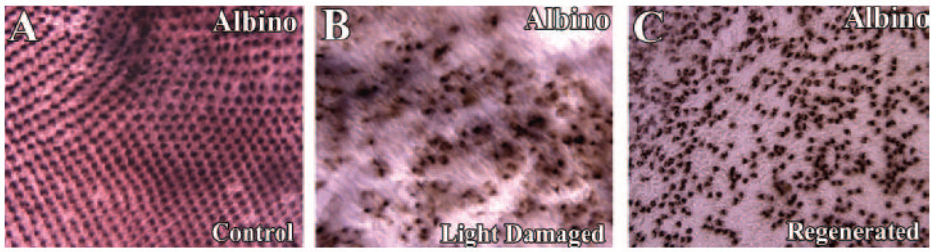

Figure 4.

Blue cone distribution in light-damaged and regenerated *alb* zebrafish retinas. Wholemount in situ hybridizations using a blue opsin cRNA probe of retinas from the following experimental groups are shown: (**A**) non–light-treated control, (**B**) 3 days intense exposure to light, and (**C**) 33 days after treatment with light. A precise blue cone mosaic was present in the control retina (**A**), although the light-damaged retina exhibited a severely disrupted blue cone mosaic, with many missing cone cells (**B**). In comparison, the regenerated retina possessed more blue cones than did the light-damaged retina, but displayed a very irregular cone cell distribution (**C**). Scale bar, 25 μm.

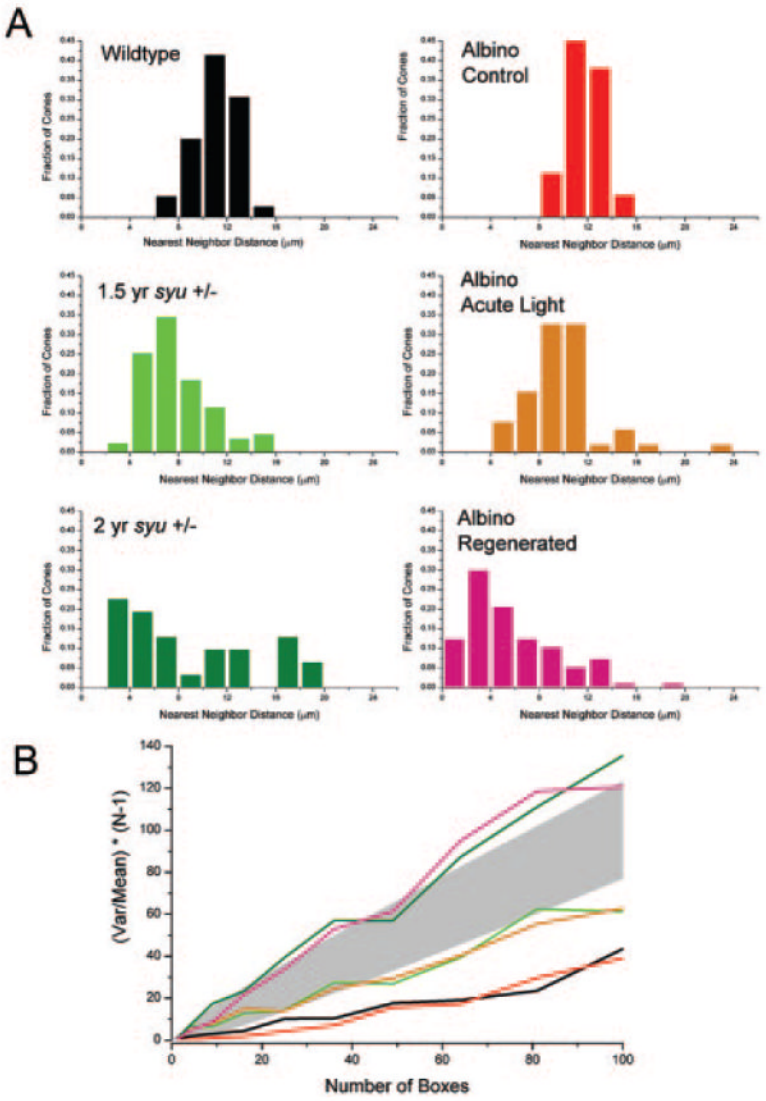

Figure 5.

Cone distributions in aged $syu^{t4+/-}$ and light-damaged and regenerated *alb* zebrafish retinas are quantitatively similar. (**A**) NND histograms reveal a normal distribution of blue cones in wild-type (*black*) and control *alb* retinas (*red*) retinas. NND distributions are less "normal" in retinas from aging $syu^{t4+/-}$ (*light* and *dark green*), light-damaged (*orange*), and the light-damaged regenerated retinas (*pink*). (**B**) Quadrat analysis of blue cone pattern in wild-type and control *alb* retinas (*black* and *red lines*, respectively) resulted in values of (var/mean)($N - 1$) that are significantly lower ($P = 0.05$ criterion) than expected for a Poisson distribution, which is consistent with a highly regular pattern. Pattern analysis of the blue cones in middle-aged $syu^{t4+/-}$ retinas (*light green line*) and *alb* retinas immediately after light-induced damage (*orange line*) showed values of (var/mean)($N - 1$) that are not significantly different from those expected for a Poisson distribution (represented by *shaded area*), which are consistent with random patterns. Analysis of the blue cone pattern in an old $syu^{t4+/-}$ retina and a light-damaged regenerated *alb* retina (*dark green* and *pink lines*, respectively) resulted in values of (var/mean) ($N - 1$) that are significantly higher than expected for a Poisson distribution, consistent with a clumped pattern.

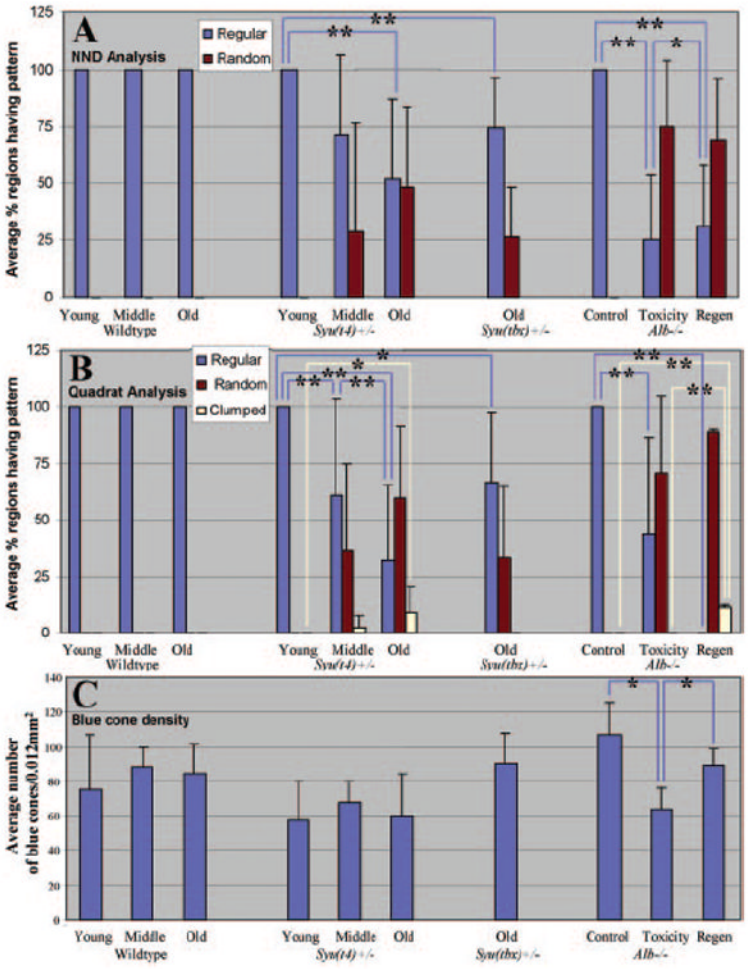

Figure 6.

Summary of blue cone pattern analyses. (**A**) Average percentage of retinal regions having regular (*blue columns*) or random (*red columns*) patterns, as determined by NND analysis. Regions were scored as significantly regular or random based on the value of the conformity ratio.[32] Proportions of regular versus random patterns were averaged over the number of retinas analyzed for each age, treatment, and genotype (two to five retinas in each case). Significant reductions in the percentage of regions showing locally regular patterns are indicated by *blue brackets* (*0.005 < P < 0.05 and **P < 0.005; Kolmogorov-Smirnov test). (**B**) Average percentage of retinal regions having regular (*blue*), random (*red*), or clumped (*yellow*) patterns as determined by quadrat analysis. Regions were scored as regular, random, or clumped based on the values of (var/mean)(N – 1).[33,35] The different proportions of each pattern type (regular, random, or clumped) were averaged over the number of retinas analyzed for each age, treatment, and genotype (two to five retinas in each case). Significant reductions in the percentage of regions showing globally regular patterns are indicated by *blue brackets* (*0.005 < P < 0.05 and **P < 0.005; Kolmogorov-Smirnov test). Significant increases in the percentage of regions showing clumped patterns are indicated by *yellow brackets* (*0.005 < P < 0.05 and **P < 0.005; Kolmogorov-Smirnov test). (**C**) Mean (±SD) planimetric density of labeled blue cones. Significant differences are indicated by blue brackets (*P < 0.05; ANOVA and post hoc analysis).

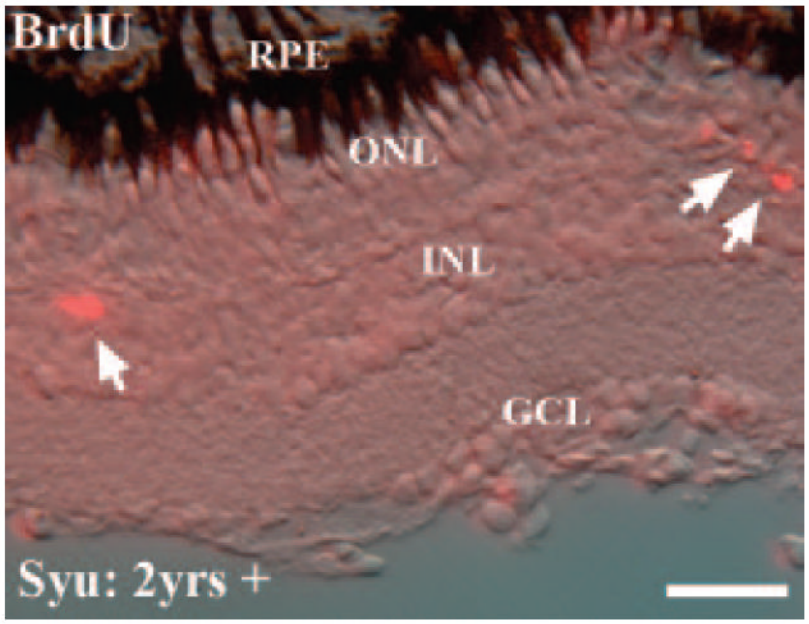

Figure 7.
Proliferating cells in the inner and outer nuclear layers of aging *syu*$^{t4+/-}$ zebrafish. Fish were systemically exposed to 5 mM BrdU for 5 days to identify dividing cells by indirect immunofluorescence with an anti-BrdU antibody. The cryosection displays the typical locations of the very few BrdU^{+} cells (*arrows*) that were observed in the oldest wild-type and *syu*$^{t4+/-}$ retinas (2 years plus). RPE, retinal pigmented epithelium; ONL, outer nuclear layer; INL, inner nuclear layer; GCL, ganglion cell layer. Scale bar, 50 μm.

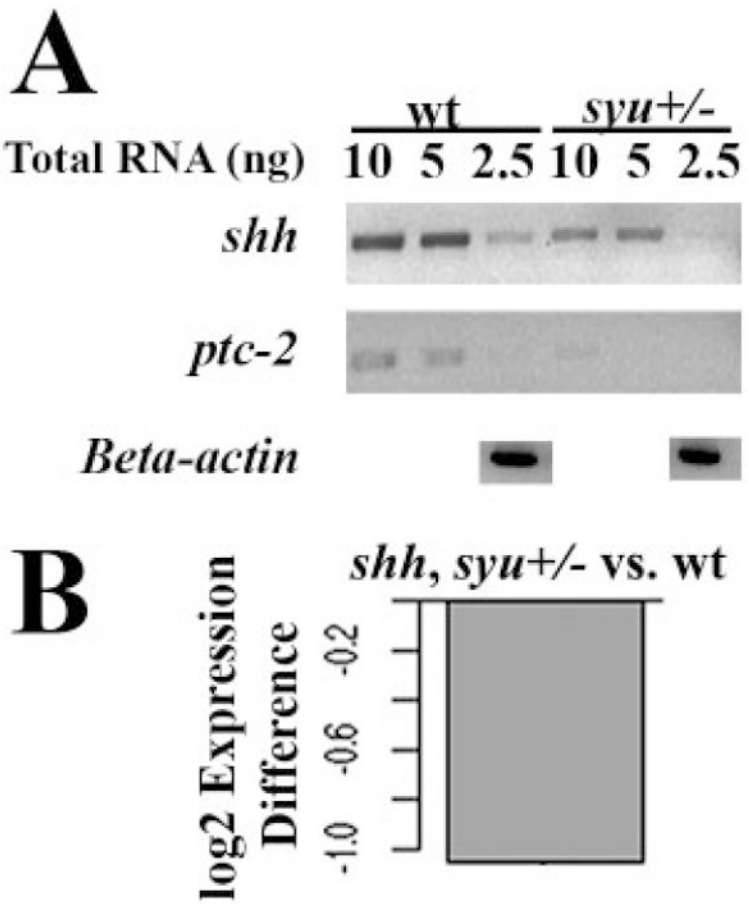

Figure 8.

Expression of *shh* and *ptc-2* mRNA in adult wild-type and $syu^{t4+/-}$ zebrafish retinas. (**A**) Semiquantitative RT-PCR of *shh* and *ptc-2*; PCR products amplified from retinas of adult $syu^{+/-}$ zebrafish and their wild-type (wt) siblings. (**B**) qRT-PCR analysis showing that expression of *shh* mRNA (normalized to that of 18s rRNA) is reduced in $syu^{+/-}$ retinas compared with wild-type.

Table 1

Cone Pattern Abnormalities Are Both Genotype-and Age-Specific

Genotype	Age	Fish (*n*)	Average of Sections Analyzed/Fish* (*n*)	Fish with Cone Loss/ Abnormality* (%)	Fish with Cone Pattern Abnormality† (%)
Wild-type (Tu and SciH)	3–10 mo	1	10	0	0
	1.5 y	5	45	0	0
	>2 y	5	45	0	0
Syu$^{t4+/-}$	3–10 mo	2	39	0	0
	1.5 y	10	39	0	75
	>2 y	12	42	50	100
Syu$^{tbx+/-}$	>2 y	4	30	0	50

*Sections: zpr-1 (red/green cone) labeling.

†Wholemounts: blue cone opsin labeling.

Table 2

Cell Death and Cell Proliferation in Wild-Type and *Syu*$^{t4+/-}$ Retinas

		TUNEL Labeling				BrdU Labeling			
				Average TUNEL$^+$ Cells/ Section (*n*)				Average BrdU$^+$ Cells/Section (*n*)	
Genotype	**Age (y)**	**Fish (*n*)**	**Average Sections Analyzed/Fish (*n*)**	**ONL**	**INL**	**Fish (*n*)**	**Average Sections Analyzed/Fish (*n*)**	**ONL**	**INL**
Wildtype (Tu and SciH)	1.5	2	5	0	0	5	27	0.5	0.3
	>2	2	5	0	0.1	5	12	0.3	0.3
Syu$^{(t4)+/-}$	1.5	6	5	0.1	0.1	6	45	0.4	0.3
	>2	6	5	0.1	0.2	7	24	0.1	0.6